Appl. Phys. B (2005)
DOI: 10.1007/s00340-005-2011-2

Applied Physics B
Lasers and Optics

B. GÜTLICH[1,✉]
H. ZIMMERMANN[1]
C. DENZ[1]
R. NEUBECKER[2]
M. KREUZER[2]
T. TSCHUDI[2]

Forcing and control of localized states in optical single feedback systems

[1] Westfälische Wilhlems Universität Münster, Institut für Angewandte Physik, Corrensstrasse 2, 48149 Münster, Germany
[2] Technische Universität Darmstadt, Institut für Angewandte Physik, Hochschulstrasse 6, 64289 Darmstadt, Germany

Received: 25 May 2005/Revised version: 2 September 2005

ABSTRACT Under feedback extended nonlinear optical systems spontaneously show a variety of periodic patterns and structures. Control gives new insight into these phenomena and it can open the way for potential application of nonlinear optical structures. We briefly review methods to control localized states in single feedback experiments. Application of a Fourier control method allows to modify interaction behavior of the localized states. As a further approach we study a forcing method, using externally created light fields as additional input to the system. Recent experiments show that the forcing method enables to favor addressing positions for localized structures. We demonstrate static addressing and favoring of addressing positions. We extend the forcing method to a dynamic forcing scheme, which allows to move and reposition localized states. Additionally forcing is used to balance experimental imperfections.

PACS 05.45.Gg; 42.60.Jf; 42.65.Tg

1 Introduction

Control of nonlinear systems is essential, firstly if one considers the use of these systems in the context of application, and secondly to increase the knowledge about the system behavior itself. Better models and better understanding of these systems can be derived from the knowledge obtained with control. Even though nonlinear systems in general exhibit very complex behavior in space and time, astonishingly simple methods can be successful in controlling the complexity of nonlinear systems. As the example of the time delayed feedback method suggested by Pyragas [1], which allows one to stabilize chaotic nonlinear oscillators to a specific system-inherent solution, powerfully demonstrates. Other control methods e.g., include Fourier-space methods, methods of stochastic resonance, at which the system is stabilized by adding noisy signals, forcing methods, in which externally generated forcing signals act on the system, or methods, which make use of synchronization effects [2–35]. Methodically one can distinguish between minimal-invasive and invasive methods. Minimal invasive control can be used to stabilize solutions already existent in the uncontrolled system. Application of minimal invasive control will results in vanishing control signals, if the target state is reached. In contrast, external target states are imposed onto the system in invasive methods, and consequently the control signals cannot vanish.

This article covers control and forcing methods applied to spatially extended optical systems. We restrict ourselves to the class of so-called single feedback systems and to therein spontaneously forming spatio-temporal optical structures [36–53]. As we deal with a spatially extended system, Fourier methods and forcing methods applied in real space are particularly well-suited to control the evolution of the transverse structures. If the Fourier- or real space control methods are made time-dependent, these spatial methods are also well-suited to control the temporal evolution of the system. In a first part we briefly review application of Fourier control and forcing methods to periodic patterns. At the example of a single feedback experiment using a liquid crystal light valve (LCLV) as nonlinearity we will, in more detail, study results on Fourier control and forcing of spatially localized states. The Fourier control method allows one to arrange localized structures, in accordance with predefined symmetries as hexagons and squares. Also the typical distances between localized states can be altered. In a novel approach we experimentally use static and dynamic forcing to demonstrate static and dynamic positioning of localized structures. Pinning positions, at which localized structures favorably form spontaneously, can be balanced by forcing and even these favorite addressing positions can be artificially selected by forcing. By varying the strength of the forcing signal forcing can also be used to address localized states. Ignition and erasure of localized states are possible. Additionally the forcing signal is used to balance experimental imperfections of the setup.

1.1 *Single feedback systems*

One reason why the class of so-called single feedback systems is often used to study the formation of spontaneous optical structures is the separability of the dominant physical processes. If the nonlinear medium can be approximated as optically thin, diffraction and optical nonlinearity are spatially well-separated effects in single feedback experiments, which simplifies theoretical and experimental treatment.

✉ Fax: +49-251-8333513, E-mail: guetlich@uni-muenster.de

These setups are called single feedback, since each wave front travels around the system once only. On the other hand also optical resonators, which provide repeated interaction between the optical wave and the nonlinear medium, are often used to study spontaneous pattern formation. A single feedback system functions in the following way: a plane pump wave is spatially (phase-) modulated by passing a nonlinear medium. The modulated wave is fed back to the nonlinear material, thereby propagating in free space over a certain distance. During propagation diffraction causes the transformation of small intrinsic modulations in the transverse phase profile into corresponding intensity modulations. This intensity profile then interacts with the plane pump wave via the nonlinear material. Many different nonlinear optical materials, such as liquid crystals [39, 40], sodium vapor [43–46], photorefractive crystals [47–49] and others have been used as optical nonlinearity. Most commonly, the optical response of the material is of the Kerr-type, i.e., the nonlinear materials alter their refractive index with the intensity. Consequently, in Kerr-type nonlinearities the intensity profile of the feedback wave causes a correspondingly induced phase profile of the next pump wave front, thus closing the feedback loop.

Commonly, a transverse modulation instability [54] arises in single feedback configurations at certain thresholds of the dominant system parameter, which results in the spontaneous self-organized formation of transverse optical structures and patterns. The wealth of observed patterns ranges from periodic patterns such as hexagons, stripes, squares, and quasi crystalline patterns [36, 40, 46–49], to spiral patterns, target patterns [50], spatio-temporally complex states and localized structures [51–53]. For these localized states also expressions like solitary structure, dissipative soliton and cavity soliton are commonly used. At first, research efforts were directed to the principal understanding of these systems. For this purpose theoretical models for the different single feedback systems have been derived and were e.g., analyzed with the help of linear stability analysis [36–38]. As straightforward analytic solutions up to now do not exist for most systems, the detailed system behavior is theoretically investigated with numerical methods.

1.2 *Fourier control methods*

Pioneer work in controlling nonlinear spatially-extended optical systems has been accomplished by making use of Fourier control methods [2, 6–16]. Comparison between numerical and experimental results points to the existence of unstable stationary solutions, which are not accessible without control. Therefore, following a suggestion from R. Martin et al. [2], a Fourier control has been applied to single feedback systems to stabilize otherwise unstable pattern solutions in the system by making use of minimal invasive techniques. The principle of the control is the following: A small fraction of the feedback wave is coupled into a control loop. Within the control loop the deviations of the feedback wave from a defined target state are detected. Thus, an error signal is created, which is coupled back negatively to the undisturbed feedback wave. In case of the Fourier control the wave coupled into the control loop is first spatially Fourier transformed. The Fourier transformed wave is filtered with an amplitude masks, which blocks the target state. The wave passing the Fourier mask thus contains only deviations from the target state. The final control signal is created by performing the inverse Fourier transformation. Control is achieved by subtracting the control wave from the feedback wave. As we deal with an optical system the subtraction can be easily realized by superposing the coherent fields of feedback and control wave with a phase shift of π. If the target state is a stable or instable stationary solution of the system, the system will move towards the target state, when the Fourier control is active. If finally the target state is reached, the control signal will vanish.

This control method has been applied in many experiments using photorefractive media, sodium vapor, or liquid crystal light valve as nonlinearity [6–16]. The experiments succeded in stabilizing otherwise unstable pattern solutions. Also the predicted vanishing of the control signal has been observed experimentally [13]. The stabilization even works in parameter regimes where the system states becomes spatio-temporally complex [13, 14] and the control induced removal of defects in the pattern has been studied [15].

The method of Fourier filtering has also been used to verify theoretical predictions such as the bifurcation diagram of unstable pattern solutions and the curve of marginal instability, which were otherwise not accessible to an experimental evaluation [17–19]. For example, the Fourier control method has been used to measure the pattern amplitude of the experimentally unstable square and roll solutions [17]. Thus the bifurcation diagram of pattern states, which are usually suppressed in favor of the hexagon solution, can be determined experimentally. The experimentally measured pattern amplitudes agree very well with the numerical predictions [17]. Also the curve of marginal instability derived with a linear stability analysis (LSA) is in general not accessible to an experimental measurement, because the small amplitude approximation used for LSA ceases its validity above threshold of the modulation instability. The curve of marginal instability can, however, be directly determined from experiment with help of a Fourier control, which is directly applied in the feedback arm. Such measurements have yet been performed with sodium vapor and photorefractive crystals as nonlinearity [18, 19].

1.3 *Forcing*

Another approach to control nonlinear systems constitutes the exertion of forcing. In this method a forcing signal is generated externally, which then acts at the nonlinear system. Mainly forcing has been investigated in context of convection pattern and in chemical reaction diffusion systems. One and two dimensional as well as static and dynamic forcing schemes have been applied to these systems [20–32]. Even if the forcing is small in comparison to the feedback signal, control of the nonlinear system can be gained. Methodically, thus, an input is offered to the system, while one studies the system's response to the input. An advantage of forcing is that not only the response to system-inherent "natural" system states can be studied, but also other external states can be offered as forcing input. The system response will however be different, if the forcing input is a solution of the unforced

system or not. It can be expected, that the system follows the forcing input, if it is a solution of the unforced system, while it remains open how the system responds to other forcing inputs. In any case forcing must be carefully adjusted to the system, as the system looses its ability to react, if the forcing is so strong, that it absolutely dominates the system behavior by itself.

In the single feedback experiment, external forcing inputs have e.g., been realized by adding small incoherent intensity distributions to the feedback [33, 34]. Static or dynamic forcing signals have been used in these experiments, while the forcing level remained small (in the order of few percent) in comparison with the feedback signal. At first forcing signals have been used which had the hexagonal symmetry of the spontaneously forming patterns. Varying the wavelength of the hexagonal forcing input, we have observed that the system follows the forcing at certain resonant forcing wavelengths, while the system is dominated by strong spatio-temporal dynamics at other wavelengths. This behavior can be interpreted as a generalized form of synchronization of a spatially extended and continuous system to a static spatial forcing input [33, 34]. In these experiments also incomplete hexagonal forcing inputs have been used. Even though the original hexagonal symmetry was hardly recognizable in the forcing input, because many pattern spots have been removed at random, the nonlinear system responds with a perfect hexagonal pattern, which locks to the forcing input. Thus, this process can be interpreted as associative completion of an incomplete forcing input. Even if the hexagonal forcing input is rotated around its center, the system perfectly follows the rotating forcing, if the velocity of rotation is not too fast [16]. Therefore also the extension of the method to dynamic forcing is possible. Now also, two independent single feedback systems were unidirectionally coupled. Both systems were in spatio-temporal complex states and it has been investigated, if the slave system follows the behavior of the master system. Synchronization of the slave system has been observed. Therefore, we have, to our knowledge, for the first time demonstrated that the concept of synchronization, previously studied at coupled networks of one dimensional oscillators, can also be extended to spatio-temporal complex system states [35].

The above-described methods of control and forcing constitute the toolbox that we now intend to use at localized states in an experiment with a liquid crystal light valve (LCLV) under optical feedback.

2 Application of control to localized states

2.1 *Localized states*

Among the wealth of transverse optical structures, localized states are of particular interest, because they can potentially be of use in context of all optical information processing. Due to their robustness and their binary features they can be interpreted as the natural binary units of nonlinear optical systems [52, 53, 55–84]. The robustness of localized states against perturbations results from their formation in a self-organized process, in which the structure of the localized state becomes a stable solution of the nonlinear system. If small perturbations occur, the system tends to relax into the stable solution, which is the localized state. Localized states, thus, posses a certain self-healing ability.

The reason for the formation of localized states is a balance between diffraction and nonlinear self-focussing. The resulting optical structure of the localized state, which combines a self-induced lens and free-space propagation, can potentially be used to guide information in context of all-optical information processing. A bistability of the feedback intensity between a stationary uniform state of the transverse intensity distribution and a stationary structured state is crucial for the formation of localized optical states in systems with optical feedback [84]. Bright localized states exist, if the uniform stationary solution is darker than the structured solution. Such a scenario can be reached either if the pattern grows from a subcritical bifurcation or if additionally to the pattern state another global bistability exists in the system. Also, bright localized states with a darker patterned state as background have been observed, if multistability exists in the system. Typically, resonators with an intra-cavity Kerr-type nonlinear medium (or another dispersive nonlinearity) exhibit the needed bistable behavior, since the resonance depends on the intra-cavity phase [71–73]. Single feedback systems can also show bistability, if e.g., the nonlinearity responds asymmetrically in respect to the polarization state of the incident wave [77, 79]. In presence of bistability, the system can realize localized states due to the coexistence of uniform dark and modulationally instable bright state. The localized state then represents a solution, which connects uniform dark and the structured upper state. Bright localized states then appear as bright spot like structures, which are generally accompanied by a self-diffraction ring structure, on top of a dark uniform background.

2.2 *Interaction*

It has been shown, that phase gradients influence the motion of localized states [61, 73, 74]. Consequently, the individual spots can be imagined to move in a phase gradient landscape, determining the final equilibrium state. This phase gradient landscape contains contributions of the mutual interaction between the spots and on the other hand a global part, which is independent of the individual spots [79].

The spot–spot interaction is related to the self-diffraction rings that are observed around localized structures. The visible intensity rings correspond to a similar phase profile, leading to attraction and repulsion of adjacent spots. Depending on their relative distance, a minimal spot distance exists, and it can be expected that neighboring spots lock on the diffraction rings even at higher orders. The resulting accumulation of localized states at corresponding locking distances has been confirmed experimentally [77, 81].

Inhomogeneities in the feedback system, such as dust particles, imperfections in the planar pump wave or a smooth spatial variation of the nonlinearity's sensitivity will also result in phase gradients. In consequence movements along these phase gradients will be induced towards either the maximum or minimum of the phase gradient [75]. The localized states are e.g., expected to move either towards or away from the beam center, if the beam profile is Gaussian. Also, for the pinning of localized states to favored positions, e.g., observed in the experiment using a liquid crystal light valve [81], small

scale spatial inhomogeneities in the phase profile can be made responsible.

If one considers the application of localized states, the control of their positioning, their interaction behavior and their movements is crucial. Thus, we investigate control methods, which potentially allow one to fulfill this task. Before we discuss the methods used to control localized states, we first introduce the experimental setup in use, a liquid crystal light valve in single feedback configuration.

2.3 *The liquid crystal light valve under optical feedback*

In the system under investigation, we use a reflective liquid crystal light valve (LCLV) as hybrid optical nonlinearity. The LCLV shows the characteristic of saturable Kerr nonlinearity. It is used because of the strong nonlinear coefficient, which allows one to achieve large aspect ratios even at moderate laser powers.

The LCLV consists of a nematic liquid crystal layer (LC) in planar alignment, a dielectric mirror and a photoconducting layer sandwiched between ITO coated glass substrates. The device, which is operated with a bias voltage applied over the transparent ITO electrodes, can be divided in two functional sides, a read and a write side. According to the intensity distribution at the photoconductive write side the birefringence of the LC read side is spatially modulated. A read wave passes the LC layer, is reflected at the dielectric mirror, and leaves the LCLV modulated in its phase and polarization state. The phase shift φ of the extraordinary wave induced by the LCLV can be written as [40, 41]:

$$\tau\partial_t\varphi - l^2\nabla_\perp^2\varphi + \varphi = \varphi_{\max}\left\{1 - \tanh^2\left(S_0\frac{\kappa_1 I_\mathrm{w}+1}{\kappa_2 I_\mathrm{w}+1}\frac{U_\mathrm{ext}-U_\mathrm{th}}{U_0}\right)\right\}. \quad (1)$$

In the equation τ is the effective response time of the LCLV and l is an effective diffusion length, which takes account of the restricted transversal resolution of the LCLV. For the LCLV in use the response time was in the order of $\tau \approx 50$ ms and the effective spatial resolution was $l \approx 30\,\mu$m. The phase shift depends on the spatial distribution of the write intensity $I_\mathrm{w}(x, y)$. U_ext is the ac voltage externally applied on the LCLV. $\varphi_{\max}$, S_0, κ_1, κ_2, U_th and U_0 are device specific fit parameters.

The LCLV is operated in a typical single feedback configuration (schematic setup see Fig. 1). As the light source a Nd:YAG laser ($\lambda = 532$ nm, $P = 100$ mW) is used. The input in the feedback loop is a linearly polarized uniform pump wave from the laser, expanded to a beam diameter of approximately 2 cm. In the central area of the expanded beam an aperture of 8 mm in diameter is cut out (A1). The direction of polarization of the pump wave includes an angle of Ψ in respect to the optical axis of the LC layer. This wave passes the read side of the LCLV, where it is reflected and modulated in its phase and polarization state according to (1). The modulated light field propagates freely over distance L. After propagation the light field is imaged by optical components (mirrors (M), lenses(L), penta prism (PP), dove prism (D), and beam splitters (BS)) to the write side of the LCLV, thus closing the feedback loop. A polarizer (P) in the feedback loop selects

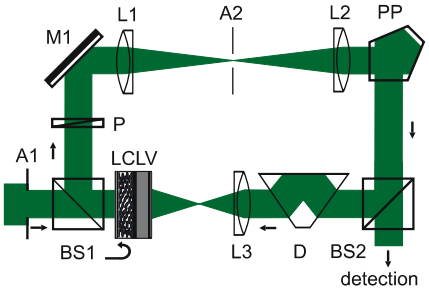

FIGURE 1 Scheme of the experimental setup: A liquid crystal light valve (LCLV) in single feedback configuration. A detailed description can be found in the text

a polarization state at $-\Psi$ in respect to the optical axis of the LCLV. A dove prism (D) is inserted to the feedback loop to correct rotational misalignment of the feedback wave.

In completion of the equation describing the response of the material ((1)), the resulting intensity I_w at the LCLV write side (photoconducting layer) can be written as:

$$I_\mathrm{w} = \left|\exp\left(\frac{-\mathrm{i}L}{2\boldsymbol{k}_\lambda}\nabla_\perp^2\right)\left(B\mathrm{e}^{-\mathrm{i}\varphi} + C\right)\right|^2 I_\mathrm{p}\,. \quad (2)$$

In this equation L accounts for the propagation length, $\boldsymbol{k}_\lambda$ is the wave vector of the light field and $\mathrm{e}^{(-\mathrm{i}L/(2\boldsymbol{k}_\lambda)\nabla_\perp^2)}$ is the propagation operator. The linearly polarized pump wave is represented by the pump intensity $I_\mathrm{p} = |E_\mathrm{p}|^2$. The pump field is phase modulated by $\mathrm{e}^{-\mathrm{i}\varphi}$. The amplitude factors $B = \cos^2\Psi$ and $C = \sin^2\Psi$ describe the influence of polarization. Phase-only modulations can be induced, if the incident wave and the polarizer in the feedback include the angle $\Psi = 0$ with the optical axis. In this case $B = 1$ and $C = 0$.

The LCLV itself provides a self-defocusing nonlinearity. Due to a symmetry in the model equations, one can simulate a self-focusing nonlinearity needed for the creation of robust localized states by using a negative propagation length [38, 39]. In the experiment, a negative propagation length is realized by imaging a virtual plane (A1) in front of the LCLV onto its photoconducting side. Experimentally the far and near field of the intensity distribution I_w are recorded by imaging fractions of the feedback wave (e.g., at beam splitter (BS2)) to a CCD camera.

2.4 *Spontaneously forming structures in the LCLV experiment*

The onset of spontaneous pattern formation is theoretically investigated with a linear stability analysis (LSA). If the intensity of the pump wave exceeds a threshold, LSA shows, that the uniform state becomes modulationally unstable against perturbations with a critical wave number k_c [36]. In consequence, stationary spatial structures evolve spontaneously with scaling in accordance to the critical wavenumber k_c. The patterns are observed as modulation of the transverse intensity distribution of the feedback wave. In the case of pure phase modulation, these are regular patterns (hexagons). If the pump intensity is increased also higher wavenumbers are excited and the patterns become increasingly disordered and also show complex spatio-temporal dynamics at even higher pump intensities.

In the case of polarization modulation, the structures can be more complex already at the threshold pump intensity [40–42, 82]. An experimental realization of bistability is found in polarization mode, and thus in polarization mode also the existence of localized states is enabled. We plot a typical plane wave bistability curve on the left hand side of Fig. 2, where the induced phase shift φ is plotted over the pump intensity I_p. Experimentally the write intensity I_w can be taken as a measure for the phase shift φ. Fractions of the curve with negative slope are unstable solutions.

On the right hand side of the figure, the curve of marginal stability, derived from a LSA, is shown, at which the system becomes unstable against perturbations with wavenumber k. At the turning points of the hysteresis curve, the system would become unstable against perturbations with $k = 0$ (dotted line). However, before reaching the plane-wave switching threshold the uniform solution becomes modulationally unstable and spontaneously forms transverse structures (dash dotted line). If one starts a numerical simulation with a uniform solution on the upper branch while decreasing the input intensity, similar behavior is observed. Before reaching the uniform threshold modulation instability sets in and transverse structures are formed. Typically localized states exist in the parameter range where the uniform dark branch coexists with a structured bright branch [42, 81, 82].

The localized states now can be generated by illuminating the LCLV's photoconducting side with a bright, random light distribution. While illuminating the system first switches to a bright state. After illumination localized states start to form. During transient states the localized structures interact. They spontaneously drift, very close structures merge, while others lock at typical distances and some simply disappear. Finally steady state configurations evolve, which can be stationary to more than half an hour. How the formation of localized structures evolves can be seen in Fig. 3. Analyzing the positions where localized states evolve, it is found that the localized states preferably form at favorite pinning positions [81]. Most likely inhomogeneities in the phase profile of the feedback wave are responsible for these favorite pinning positions. These inhomogeneities in the phase profile can either result from imperfections in the imaging system such as dust particles or small misalignments in the beam path or result from spatially inhomogeneous response of the LCLV.

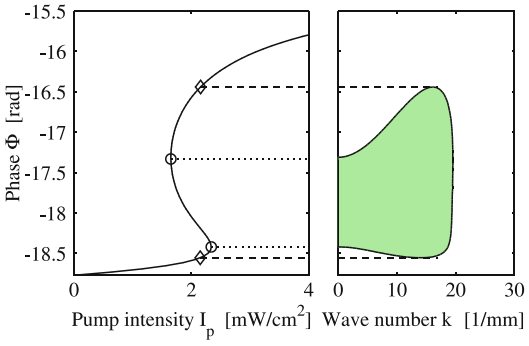

FIGURE 2 Results of a linear stability analysis (*right hand side* of the image) and the corresponding plane wave solution (*left hand side* of the image). The uniform solution becomes unstable against perturbations with wave number k in the grey shaded area. The plot of the plane wave solution shows the hysteresis behavior of the system (negative slopes are unstable solutions), which results in a bistability of the system. Included in the plot are thresholds, where the lower and higher branch of the plane wave solution (○) become modulationally unstable and where the uniform solutions becomes unstable against $k = 0$

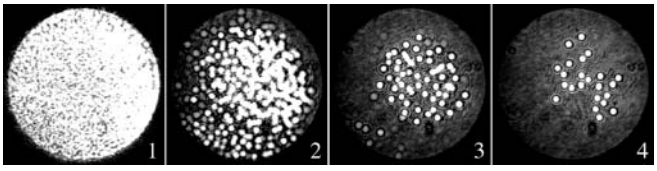

FIGURE 3 Creating localized structures by illumination with white light. The system switches to a broadly excited solution (image (**1**)). Solitary spots form while interacting with each other ((**2**)–(**3**)). After some seconds steady states form (**4**). Beam aperture: $d = 8$ mm; propagation length $L = -13$ cm

3 Fourier control of localized states

In the following, we are going to apply the Fourier control scheme to control the localized states. We expect the localized structures to rearrange themselves in accordance to the symmetry and the distances determined by Fourier control. In this respect, low pass filtering directly in the feedback arm has already been used to alter the locking distances between localized states [83]. This result makes the application of a control scheme in Fourier space promising to now also modify the symmetry of interaction.

3.1 *Experimental setup: Fourier control*

Experimentally the Fourier control is realized all optically by adding a control arm (marked area in the scheme of the control setup in Fig. 4) to the feedback. At the beam splitter (BS2), a fraction of the light wave is coupled from the feedback into the control arm. The feedback wave is imaged to the LCLV's write side, without alteration by reflection at a mirror and the beam splitter.

Within the control arm, a Fourier transformation and its inverse operation are performed optically by lenses in a $4f$-configuration. The Fourier filtering is realized at the focal plane between the lenses, where a amplitude mask is placed. The Fourier transformed wave passes the Fourier mask (F), where the target state is blocked. Afterwards the control signal, which now consists of the deviations from the target state,

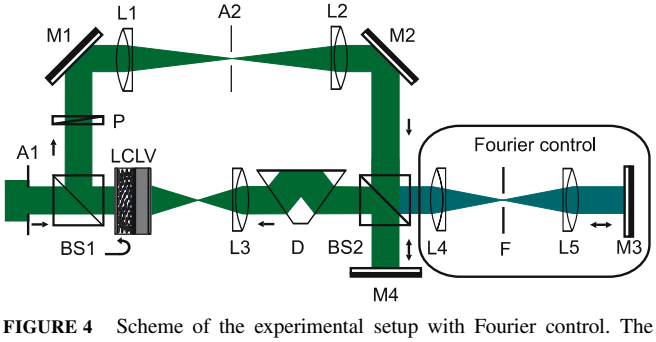

FIGURE 4 Scheme of the experimental setup with Fourier control. The light wave splits into a feedback arm and a control arm at a beam splitter (BS2). The control signal is created with the help of Fourier masks (F), which block the target state. At the beam splitter (BS2) control signal and feedback signal interfere destructively, which is equivalent to a subtraction. (a more detailed description can be found in the text)

is inversely Fourier transformed, reflected at the mirror at the end of the control arm and therefore passes the Fourier masks twice.

The combination of feedback arm and control arm form an interferometer of the Michelson type. The phase difference between control and feedback can be adjusted, such that destructive interference over the complete aperture is yielded. This condition is equal to the subtraction of the control wave from the feedback wave. The strength of the control $s^2 = I_{\text{control}}/I_{\text{feedback}}$ can be altered by changing the fraction between intensity of the control signal, in respect to the feedback wave.

Note, that in the case of localized structures, a much broader band of wave numbers in k-space can be excited than in the case of patterns where only the critical wave number k_c or distinct higher orders are excited. To position localized states closer than $1/k_c$, which determines their structure size, is not sensible, because it will result in the merging of localized structures. Therefore we use control at wave numbers $k < k_c$. The masks were designed such that they block the wave number k_{mask} as fundamental mode. Fourier components equivalent to modes of a square grid and a hexagonal grid were chosen. To make certain that the zeroth order, which contains the largest fraction of intensity, is completely blocked and in order to simplify experimental adjustment the central spot of the mask was designed slightly larger than the other spots.

3.2 *Results: Fourier control*

From the start it was not obvious how localized states would behave with control applied. Especially the danger to suppress localized structures by control could not be excluded, because the control favors the Fourier modes of the target state, while it suppresses all other modes.

If carefully adjusting control such that suppression of modes essential for the existence of localized states was avoided, Fourier control enables one to position localized structures in accordance to target grids with hexagonal and square geometry in experiment (Fig. 5). As before localized structures have been addressed by an inhomogeneous illumination of the LCLV's write side, while now the Fourier control was active. In the experiments a propagation length of $L = -10\,\text{cm}$ was used and the voltage applied on the LCLV was $U_{\text{ext}} = 7.5\,V_{\text{pp}}$. The beam aperture was 8 mm wide and the control strength set to $s^2 \approx 3\%$. Two different scales of the Fourier masks were used experimentally. The masks selected either a square or hexagonal target symmetry at two different wave numbers, namely $k_{\text{mask}} = 13\,\text{mm}^{-1}$ and $k_{\text{mask}} = 10\,\text{mm}^{-1}$, in Fourier space. An estimation of the critical wave number k_c, which neglects diffusion [38, 40], yields $k_c = 2\pi/\sqrt{2\lambda L} = 19\,\text{mm}^{-1}$ for the parameters used in experiment. The typical minimal distances between localized states change to the distance selected with the controlling scheme. Using $k_{\text{mask}} = 10\,\text{mm}^{-1}$ a minimal distance between the localized states of $d_m = 630\,\mu\text{m}$ was observed, while the minimal distance changed to $d_m = 480\,\mu\text{m}$, when $k_{\text{mask}} = 13\,\text{mm}^{-1}$ was used. Also the localized structures arrange themselves in accordance with the symmetry selected by Fourier control [81].

For comparison also numerical simulations have been performed using the model described by (1) and (2). The numerical findings are in agreement with the experiment. However it was observed that starting from a small number of localized states addressed as initial states a patterned domain consisting of localized structures grows, when control is applied (Fig. 6). As reason for the growth of the patterned domain we suggest a process which involves the changed diffraction ring structure. Due to active control, the diffraction ring changes from the typical circular structure to a square or hexagonal structure depending on the control symmetry. Simultaneously with these modifications, the localized structures attract each other. This causes the superposition of the modified ring structure. The intensities are higher exactly at the intersection positions, which agree with empty places of the hexagonal or square grid. Thus the application seems to induce the ignition of new localized states exactly at places between interacting localized structures. As can also be seen in the evolution, noninteracting single localized states are not involved in this process.

In the experiment the numerically observed growth of patterned domains could not clearly be confirmed, due to the sensitivity of the Michelson interferometer, which is formed by the feedback and control loop, to vibrations and disturbances. The disturbances of the interferometer result in a drift of phase difference between feedback and control loop and

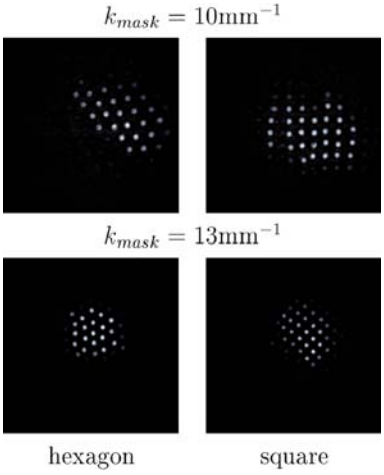

FIGURE 5 Experimental images of controlled localized structures. Fourier control orders localized structures in square and hexagonal symmetries with different typical distances between the structures. Beam aperture: 8 mm; propagation length $L = -10\,\text{cm}$

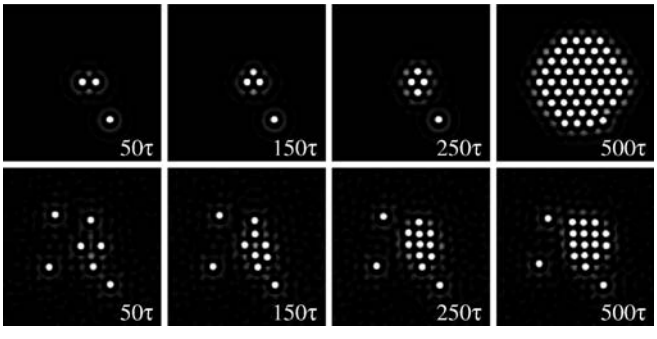

FIGURE 6 Numerical simulations with hexagonal (*1. row*) and square (*2. row*) control. The control forces solitary spots to arrange in accordance to the control grid. New spots get switched on at edges and on gap positions

therefore lead to a change from destructive to constructive interference. If constructive interference occurs, the control is deactivated and the deviations from the target state are even amplified in the system. Additionally, constructive interference results in an increase of the write intensity and consequently localized structures can be generated spontaneously. Due to this instability of the interferometer it was not possible to address localized structures individually. Instead a broad random intensity distribution has been used to address localized structures, while control was already active. Therefore, the control induced evolution of individual localized structures has not yet been studied. In consequence it is difficult to compare numerical and experimental findings in that respect.

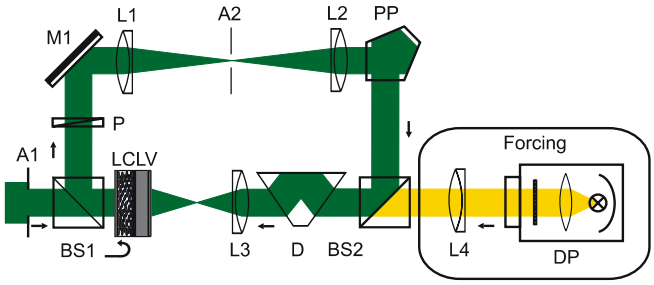

FIGURE 7 Scheme of the experimental setup with forcing. The forcing input is created with a data projector (DP) as an incoherent white light intensity distribution. The forcing input is added to the feedback signal by projecting it to the photoconducting side of the LCLV with a lens (L4)

4 External forcing

A principal disadvantage of Fourier methods, if applied to localized states, is the global action on distinct spatial modes. Consequently the positions of localized states can only be controlled relative to each other. However, an exact spatial positioning would be required in context of potential application. To achieve such an absolute positioning control must be applied in real space. In order to allow for the necessary flexibility and adaptability to the control needs, we now investigate application of an external forcing method to control localized states. The forcing input can be arbitrarily designed and also the creation of dynamic forcing schemes is possible. As forcing input we are going to generate spatial intensity distributions, which we will incoherently add to the feedback system. The response of the system and particularly of the localized states is then studied. As we use purely optical input to the system, one can interpret the suggested scheme as all-optical control of the nonlinear system. Also we do not give up the system -inherent degrees of freedom, as we do not introduce any pixelation into the feedback loop.

4.1 *Experimental setup: forcing*

To implement the forcing into the single-feedback setup, a digital LC data projector (DP) has been used (schematic setup in Fig. 7). Gray scale images, intended as arbitrary forcing inputs, were created on a PC and have been used as input for the display of the data projector. The resulting intensity distribution from the LC display is then projected to the photoconducting side of the LCLV with the help of a lens (L4). In front of the beam splitter, which couples the forcing input to the ordinary feedback loop, two polarizers and neutral density filters are placed. The first polarizer selects the green fraction of the RGB-signal from the projector. The strength of forcing can be adjusted in three ways. Firstly the combination of neutral density filters can be changed. Secondly the transmission of the second polarizer can be modulated by changing the rotation angle of the polarizer. Thirdly the grey scale values of the forcing input can be modified. For the forcing experiments, a LCLV from another producer, which shows higher sensitivity than in the Fourier control experiments, has been used. Thus, the LCLV was operated for the following experiments at a bias voltage of $U_{\text{ext}} = 6.5\,\text{V}_{\text{pp}}$. The pump intensity was set to $I_{\text{p}} = 39\,\text{mW/cm}^2$.

The additional incoherent light distribution from the forcing input results in a local offset of the induced phasemodulation φ ((1)). The consequences of this offset are twofold: Firstly the "working point" of the LCLV is locally shifted and thus the LCLV's sensitivity is locally modified. This effect can be used to compensate for inhomogeneity and also to address localized states. Secondly the local offset in phase φ can be used to create a landscape of the phase gradient. As mentioned above localized structures move towards maxima (or minima) of a phase gradient. Thus, dynamic and static positioning of localized states is enabled according to the modified phase profiles.

4.2 *Balancing experimental imperfections*

As mentioned above experimental imperfections, such as dust particles, imperfections in the planar pump wave, or a smooth spatial variation of the nonlinearity's sensitivity influence the positions of the localized states through induced phase gradients. In the LCLV experiment one of the major imperfections represents the non-homogeneous spatial sensitivity function of the LCLV. These smooth modulations in sensitivity are mainly caused by inhomogeneities in layer thickness due to imperfections in the fabrication of the LCLV's layer structure. Due to these variations the induced phase shift φ (1) varies smoothly in space. This variation is not included in the numerical model described in (1). It can however be included, if one makes either the maximal phase shift φ_{max} or the fit parameters S_0, κ_1, κ_2 space-dependent. In first approximation the central area of the LCLV's aperture seems to be more sensitive than the margins. The resulting inhomogeneities in sensitivity hinder the existence of localized structures in some areas, as localized states react more sensitive against these inhomogeneities than it e.g., seems to be the case for periodic patterns.

We now experimentally determine the spatial distribution of the sensitivity function of the LCLV and intend to use the inverted sensitivity function as forcing input to balance these modulations in sensitivity. The inverted sensitivity function has been determined by steadily increasing the intensity of a uniform forcing input. For this purpose, we altered the grey scale values of the input images. If the sensitivity of the LCLV was homogeneous, localized structures would ignite over the whole aperture at the same forcing intensity level. The intensity levels at which localized states ignite, however, vary from space to space. We now take the local intensity level at which a localized structure ignites as a measure for the LCLV's sensitivity at this position. The inverse of this result-

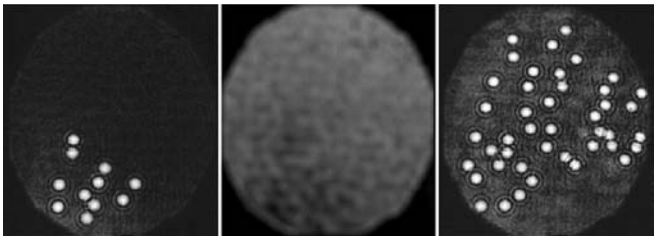

FIGURE 8 Compensation of inhomogeneous sensitivity: (*left*) System without compensation. (*center*) Inverse sensitivity function of the system. (*right*) System with compensation. The region of existence with compensation is extended. Diameter of the aperture: 8 mm

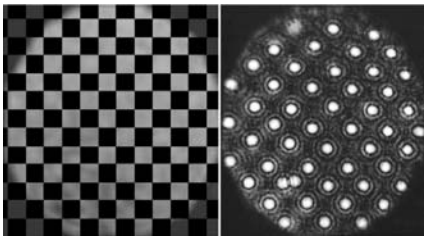

FIGURE 9 Using a chess board pattern (*left*) as static forcing input to position localized states (*right*). The individual localized states can remain bistable depending on the forcing intensity. Diameter of the aperture: 8 mm

ing sensitivity function (depicted in the center of Fig. 8) then has been used as the forcing input, which was added incoherently to the feedback signal in order to compensate for the inhomogeneities. The areas outside the aperture (A1) have been set to zero. By adding the inverted sensitivity function as forcing input, the system thus experiences an additional phase shift in regions where the induced phase shift without compensation is smaller than in the more sensitive areas. Finally, if the compensation is applied, the intensity level and contrast of the forcing input are adjusted such that a homogeneous system response is achieved, while the system remains below the switching threshold for igniting localized structures. As the experimental images in Fig. 8 show, the method allows one to compensate for the inhomogeneities in sensitivity.

With forcing used as compensation almost the whole aperture can be used to address bistable localized structures instead of only a small area. Compare the area, where stationary bistable localized states exist, without compensation (left hand side of Fig. 8) with the area of existence in the compensated system (right hand side of Fig. 8). Therefore an increased homogeneity of the experimental setup has been achieved with this method.

4.3 *Static addressing and positioning*

Depending on the strength of the forcing input, forcing also can be used to favor addressing positions or to address localized structures. To demonstrate this possibility, we multiply a chess board pattern, which varies from zero in black areas to one in its bright fields, with the compensation function, derived above in Sect. 4.2, and use the resulting intensity distribution as forcing input (left hand side of Fig. 9). If the strength of the forcing input is adjusted such that the intensity level at the photoconducting side of the LCLV, which consists of the feedback intensity and the forcing signal, remains below the switching thresholds for localized states, the forcing favors addressing positions. The system keeps its local bistability and individual localized states can be ignited. However, instead of forming at randomly distributed spontaneous pinning positions, favorably they now ignite at the positions selected by the forcing signal, which are the bright positions of the chess board pattern. In the right-hand-side image of Fig. 9, this favoring of positions can be observed. To create this image the forcing and the pump intensity have been kept at a constant level, while the photoconducting write side has been briefly uniformly illuminated to address localizes structures. As can be seen localized states form at the positions, which coincide with the chess board geometry. However small distortions from a perfect square grid are observed in the positioning of localized structures. One reason for these distortions are imperfect imaging properties of the optical system used for the projection of the forcing input. Only one lens was used for the projection of the forcing input. The observed aberrations would be minimized, if a more complex design for the projection was used. Another reason for distortions in the square grid is a certain degree of freedom in movement, which the localized states still possess within one field of the chess board. In further steps, this can be adjusted more precisely by changing the size of the chess board fields. At one grid position in the lower left-hand corner two localized structures coexist at one chess board position. At this position the forcing induced favoring did not work perfectly. This imperfection may be caused by a local imbalance of the interplay between the strength of forcing, compensation and input intensity. We additionally observed indications that localized states addressed at positions not selected by the forcing input tend to move towards the positions favored by forcing. However, we have not yet evaluated the exact motion. If the intensity of the forcing input is higher than the switching threshold of localized states, the use of forcing results in the addressing of localized states.

If the pump intensity level from the laser is chosen just below the parameter region of bistability, localized states do not form spontaneously. Addition of the square forcing signal can shift the system state into the bistable domain, while still no localized states form spontaneously. If adding another light signal, we observe ignition of localized states only at positions where the forcing input and additional switching light add. Localized states do not form at the dark areas of the chess board and at positions not illuminated by the additional switching light. Thus, this situation can be interpreted as the realization of an all optical AND. Also, if we decrease the intensity in the bright regions of the square forcing input, we observe, that individual localized structures can be switched off. In the LCLV setup yet erasing of localized structures has only been demonstrated by superposing an addressing beam, which was π out of phase with the feedback. Therefore, we developed an erasure method, which does not require coherent switching beams.

4.4 *Dynamic positioning*

In preliminary experiments also the possibility of dynamic positioning enabled by the forcing method is demonstrated. First indications of this possibility are the movements

of localized states from off site chess board positions to on site positions. In another experiment we extend the forcing method to a dynamic method in order to reposition the localized states. For this experiment a film with a moving chess board pattern has been created. (The chess board pattern at the left hand side of Fig. 9 was used.) In the film the chess board slides continuously from right to left. The film was used as forcing input. Results of this experiment are shown in Fig. 10. In the image sequence only a fraction of the aperture is shown. Localized states are addressed in a region near to the right border of the aperture, because here the intensity level of forcing was slightly above the switching threshold for localized structures. While the chess board forcing moves to the left, also the localized states move in this direction. As reference for the movement two lines have been added to the image sequence. The reference line on the right is fixed, while the reference line on the left indicates the position of the moving chess board. From the movement of localized states we conclude that the steep phase gradient, induced by the border between the chess board sections, if moved, pushes the localized states. Yet dynamic positioning only works in a comparatively small area of the beam aperture. In other sections we yet observe erasure of localized states, brief sticking of localized states to spontaneous pinning positions before they continue their movement and spontaneous interactions between localized states. Suppression of these effects can however be achieved, if the intensity of forcing strength is more carefully adjusted in respect to the pump intensity and to the strength of the compensation signal. Also the homogeneity achieved with the compensation can still be improved. However the experiments demonstrate the ability of forcing to move and reposition individual localized structures in a yet unknown way.

5 Conclusion

In conclusion we have demonstrated that Fourier control and forcing are powerful tools, which allow one to control localized structures in the LCLV system under optical feedback. Fourier control alters the interaction behavior of localized states. The localized states arrange themselves in accordance to the target geometry and in accordance to the target distances. Absolute positioning can be achieved by forcing methods. Adding incoherent white light intensity distributions to the feedback systems allows one to compensate for experimental imperfections. It can create artificial pinning positions, where localized states favorably form and to which they tend to move. If forcing intensity is adjusted appropriately to the pump intensity, an all optical and can be realized with the forcing. Also forcing can be used to address localized structures. Additionally we also demonstrate that dynamic forcing inputs can be used to dynamically position localized structures. We hope that, in further experiments, the control methods that we applied to the LCLV experiment can be also used in other contexts. In particular the application of these methods in systems, which use materials with fast response times such as active and passive resonators with semiconductors as nonlinear material, would be interesting.

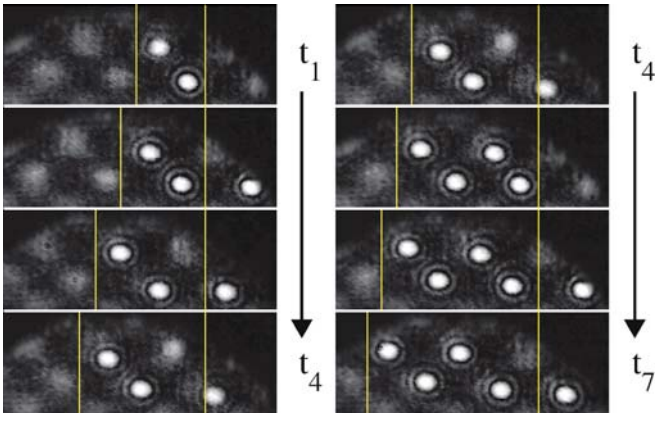

FIGURE 10 Sequence with dynamic positioning of localized states. A section of the aperture is shown. The localized states are addressed on the right, while the forcing input, which is a chess board pattern, moves to the left. The localized states follow the dynamic forcing input. Two *reference lines* illustrate the movement. The *reference line* on the *right* is fixed, while the *line* on the *left* indicates the movement of the forcing input

ACKNOWLEDGEMENTS The authirs acknowledge partial financial support from the FAZIT-Stiftung and from the DFG Graduiertenkolleg 'nichtlineare kontinuierliche Systeme'. The authors also would like to thank Prof. Dr. W. Lange, Institut für Angewandte Physik, Universität Münster, for his continuous support and for his pioneering activities in the field of transverse nonlinear optics. As members of the same institute we are especially grateful for his advice, encouragement and farsighted, prudential companionship throughtout the years of common activities at Münster.

REFERENCES

1 K. Pyragas, Phys. Lett. A **181**, 203 (1993)
2 R. Martin, A.J. Scroggie, G.-L. Oppo, W.J. Firth, Phys. Rev. Lett. **77**, 4007 (1996)
3 L. Gammaitoni, P. Hänggi, P. Jung, F. Marchesoni, Rev. Mod. Phys. **70**, 223 (1998)
4 A. Pikovsky, M. Rosenblum, J. Kurths, *Synchronization* (Cambridge University Press, Cambridge 2001)
5 I. Wedekind, U. Parlitz, Int. J. Bifurcat. Chaos **11**, 1141 (2001)
6 A. V. Mamaev, M. Saffman, Phys. Rev. Lett. **16**, 3499 (1998)
7 S.J. Jensen, M. Schwab, C. Denz, Phys. Rev. Lett. **81**, 1614 (1998)
8 C. Denz, P. Jander, M. Schwab, O. Sandfuchs, M. Belic, F. Kaiser, Ann. Phys. **13**, 391 (2004)
9 Y. Hayasaki, H. Yamamoto, N. Nishida, Opt. Commun. **187**, 49 (2001)
10 E.V. Degtiarev, M.A. Vorontsov, J. Opt. Soc. Am. B **12**, 1238 (1995)
11 T. Ackemann, B. Giese, B. Schäpers, W. Lange, J. Opt. B: Quantum S. O. **1**, 70 (1999)
12 G.K. Harkness, G.-L. Oppo, E. Benkler, M. Kreuzer, R. Neubecker, T. Tschudi, J. Opt. B: Quantum S. O. **1**, 177 (1999)
13 E. Benkler, M. Kreuzer, R. Neubecker, T. Tschudi, Phys. Rev. Lett. **84**, 879 (2000)
14 G.K. Harkness, G.-L. Oppo, R. Martin, A.J. Scroggie, W.J. Firth, Phys. Rev. A **58**, 2577 (1998)
15 R. Neubecker, E. Benkler, R. Martin, G.-L. Oppo, Phys. Rev. Lett. **91**, 113 903 (2003)
16 R. Neubecker, *Pattern Formation in an Opitcal Exeriment: From Fundametals to Applications.* Volume 115 of Reihe Physik (Tectum Verlag, Marburg 2004)
17 R. Neubecker, E. Benkler, Phys. Rev. E **65**, 066 206 (2002)
18 M. Pesch, E. Große Westhoff, T. Ackemann, W. Lange, Phys. Rev. E **68**, 016 209 (2003)
19 O. Kamps, P. Jander, C. Denz, Phys. Rev. E **72**, 016 215 (2005)
20 H.R. Brandt, Phys. Rev. A **32**, 3551 (1985)
21 P. Coullet, Phys. Rev. Lett. **56**, 724 (1986)
22 C. Elphick, J. Phys. A **19**, 1877 (1986)
23 P. Coullet, C. Elphick, D. Repaux, Phys. Rev. Lett. **58**, 483 (1987)
24 P. Coullet, D. Repaux, Europhys. Lett. **3**, 573 (1987)
25 R. Schmitz, W. Zimmermann, Phys. Rev. E **53**, 5993 (1996)
26 C. Utzny, W. Zimmermann, M. Bär, Europhys. Lett. **57**, 113 (2002)
27 L.M. Pismen, Phys. Rev. Lett. **59**, 2740 (1987)

28 P. Coullet, D. Walgraef, Europhys. Lett. **10**, 525 (1989)
29 O. Steinbock, V. Zykov, S.C. Müller, Nature (London) **366**, 322 (1993)
30 V. Petrov, Q. Oyang, H. L. Swinney, Nature **388**, 655 (1997)
31 M. Dolnik, A.M. Zhabotinsky, I. R. Epstein, Phys. Rev. E **63**, 026 101 (2001)
32 J. Wolff, A.G. Papathanasiou, I.G. Kevrekidis, H.H. Rotemund, G. Ertl, Science **294**, 134 (2001)
33 R. Neubecker, A. Zimmermann, Phys. Rev. E, **65**, 035 205 (2002)
34 R. Neubecker, O. Jakoby, Phys. Rev. E **67**, 066 221 (2003)
35 R. Neubecker, B. Gütlich, Phys. Rev. Lett. **92**, 154 101 (2004)
36 W.J. Firth, J. Mod. Opt. **37**, 151 (1990)
37 G. D'Alessandro, W.J. Firth, Phys. Rev. Lett. **66**, 2597 (1991)
38 G. D'Alessandro, W.J. Firth, Phys. Rev. A **46**, 537 (1992)
39 E. Ciaramella, M. Tamburrini, E. Santamato, Appl. Phys. Lett. **63**, 1604 (1993)
40 R. Neubecker, G.-L. Oppo, B. Thüring, T. Tschudi, Phys. Rev. A **52**, 791 (1995)
41 B. Thüring, R. Neubecker, M. Kreuzer, E. Benkler, T. Tschudi, Asian J. Phys. **7**, 453 (1998)
42 F.T. Arecchi, S. Boccaletti, S. Ducci, E. Pampaloni, P.L. Ramazza, S. Residori, J. Nonlinear Opt. Phys. Mater. **9**, 183 (2000)
43 G. Giusfredi, J.F. Valley, R. Pon, G. Khitrova, H.M. Gibbs, J. Opt. Soc. Am. B **5**, 1181 (1988)
44 T. Ackemann, W. Lange, Appl. Phys. B **72**, 21 (2001)
45 T. Ackemann, Y. A. Logvin, A. Heuer, W. Lange, Phys. Rev. Lett. **75**, 3450 (1995)
46 A. Aumann, T. Ackemann, E. Große Westhoff, W. Lange, Phys. Rev. E **66**, 046 220 (2002)
47 F.T. Arecchi, Physica D **51**, 450 (1991)
48 C. Denz, M. Schwab, M. Sedlatschek, T. Tschudi, T. Honda, J. Opt. Soc. Am. B **15**, 2057 (1998)
49 M. Schwab, C. Denz, M. Saffman, Appl. Phys. B **69**, 429 (1999)
50 F. Huneus, B. Schäpers, T. Ackemann, W. Lange, Appl. Phys. B **76**, 191 (2003)
51 A.J. Scroggie, W.J. Firth, G.S. McDonald, M. Tlidi, R. Lefever, L.A. Lugiato, Chaos Soliton. Fract. **4**, 1323 (1994)
52 G.S. McDonald, W.J. Firth, J. Mod. Optic. **37**, 613 (1990)
53 N.N. Rosanov, G.V. Khodova, J. Opt. Soc. Am. B **7**, 1057 (1990)
54 M.C. Cross, D. Hohenberg, Rev. Mod. Phys. **65**, 851 (1993)
55 D.W. McLaughlin, J.V. Moloney, A.C. Newell, Phys. Rev. Lett. **51**, 75 (1983)
56 D.W. McLaughlin, J.V. Moloney, A.C. Newell, Phys. Rev. Lett. **54**, 681 (1985)
57 Y.I. Balkarei, M.G. Evtikhov, J.V. Moloney, Y.A. Rzhanov, J. Opt. Soc. Am. B **7**, 1298 (1990)
58 G.S. McDonald, W.J. Firth, J. Opt. Soc. Am. B **7**, 1328 (1990)
59 M. Tlidi, P. Mandel, R. Lefevers, Phys. Rev. Lett. **73**, 640 (1994)
60 L. Torner, C.R. Menyuk, W.E. Torruellas, G.I. Stegeman, Opt. Lett. **20**, 13 (1995)
61 W.J. Firth, A.J. Scroggie, Phys. Rev. Lett. **76**, 1623 (1996)
62 C. Etrich, U. Peschel, F. Lederer, Phys. Rev. Lett. **79**, 2454 (1997)
63 B.A. Samson, M.A. Vorontov, Phys. Rev. A **56**, 1621 (1997)
64 W.J. Firth, G.K. Harkness, Asian J. Phys. **7**, 665 (1998)
65 M. LeBerre, A.S. Patrascu, E. Ressayre, A. Tallet, Phys. Rev. A **56**, 3150 (1997)
66 M. Segev, G.C. Valley, Phys. Rev. Lett. **73**, 3211 (1994)
67 G.I. Stegman, M. Segev, Science **286**, 1518 (1999)
68 C. Denz, W. Krolikowski, J. Petter, C. Weilnau, T. Tschudi, M.R. Belic, F. Kaiser, A. Stepken, Phys. Rev. E **60**, 6222 (1999)
69 J. Petter, J. Schröder, D. Träger, C. Denz, Opt. Lett. **28**, 438 (2003)
70 M. Peccianti, G. Assanto, Optics Lett. **26**, 1690 (2001)
71 M. Brambrilla, L.A. Lugiato, F. Prati, L. Spinelli, W.J. Firth, Phys. Rev. Lett. **79**, 2042 (1997)
72 L. Spinelli, G. Tissoni, M. Brambrilla, F. Prati, L.A. Lugiato, Phys. Rev.A **58**, 2042 (1998)
73 V.B. Taranenko, K. Staliunas, C.O. Weiss, Phys. Rev. A **56**, 1582 (1997)
74 M. Tlidi, A.G. Vladimirov, P. Mandel, IEEE J. Quantum Electron. **39**, 216 (2003)
75 A.J. Scroggie, J. Jeffers, G. McCartney, G.-L. Oppo, Phys. Rev. E **71**, 046602 (2005)
76 T. Ackemann, A. Heuer, Y. A. Logvin, W. Lange, Phys. Rev. A **56**, 2321 (1997)
77 B. Schäpers, M. Feldmann, T. Ackemann, W. Lange, Phys. Rev. Lett. **85**, 748 (2000)
78 B. Schäpers, T. Ackemann, W. Lange, J. Opt. Soc. Am. B **19**, 707 (2002)
79 M. Kreuzer, B. Thüring, T. Tschudi, Asian J. Phys. **7**, 678 (1999)
80 A. Schreiber, B. Thüring, M. Kreuzer, Opt. Commun. **136**, 415 (1997)
81 B. Gütlich, R. Neubecker, M. Kreuzer, T. Tschudi, Chaos **13**, 239 (2003)
82 P.L. Ramazza, S. Ducci, S. Boccaletti, F.T. Arecchi, J. Opt. B: Quantum S. O. **2**, 399 (2000)
83 P.L. Ramazza, E. Benkler, U. Bortolozzo, S. Boccaletti, S. Ducci, F.T. Arecchi, Phys. Rev. E **65**, 066 204 (2002)
84 P.L. Ramazza, S. Boccaletti, U. Bortolozzo, F.T. Arecchi, Chaos **13**, 335 (2003)